Influence of Outer-Shell Metal Ligands on the Structural and Electronic Properties of Horse Liver Alcohol Dehydrogenase Zinc Active Site

Francesco Luigi Gervasio,[†,‡,§] Vincenzo Schettino,[†,||] Stefano Mangani,[⊥] Matthias Krack,[§] Paolo Carloni,[*,‡] and Michele Parrinello[§,#]

Dip. di Chimica, Università di Firenze, via della Lastruccia 3, I-50019 Sesto Fiorentino, Italy, European Laboratory for Non linear Spectroscopy (LENS), via Nello Carrara 1, I-50019 Sesto Fiorentino, Italy, International School for Advanced Studies (SISSA/ISAS) and INFM-DEMOCRITOS Center for Numerical Simulation, via Beirut 4, I-34014 Trieste, Italy, Dip. di Chimica, Università di Siena, via A. Moro, I-53100 Siena, Italy, CSCS-Centro Svizzero di Calcolo Scientifico, Via Cantonale, Galleria 2,CH-6928 Manno, Switzerland, and Physical Chemistry, ETH Hönggerberg HCI, CH-8093 Zurich, Switzerland

Received: November 26, 2002; In Final Form: April 24, 2003

An analysis of the high resolution 3D structures of zinc enzymes shows that the Zn−His−carboxyl(ate)−HX (X = OH or NH) H-bond motif is common. We investigate here the influence of this motif in the active site of horse liver alcohol dehydrogenase, which features the Zn−His−Asp−H_2O motif. Density functional theory calculations are carried out on models of the active site complexed with the NAD+ cofactor, in which the metal ion binds either the alcohol substrate [Bahnson et al. *Proc. Natl. Acad. Sci. U. S.A* **1997**, *94*, 12797−12802][1] or a water molecule [Meijers et al. *J. Biol. Chem.* **2001**, *276*, 9316−9321].[2] Our calculations suggest that in both complexes the presence of Asp49 significantly affects the structural and electronic properties of the metal site. Furthermore, they show that inclusion of the Asp bound water molecule is required to describe the energetics correctly. Finally, they suggest that the Asp49/water pattern could play a role in the enzymatic reaction.

Introduction

Specific and conserved structural motifs found in enzymatic active sites but not directly involved in the catalysis may play an important role in tuning the enzymatic activity.[3] In serine proteases, for instance,[4,5] the enzymatic reaction is believed to be assisted by the hydrogen bond interaction of Ser195, the residue directly involved in the catalysis, with a histidine residue (His57), which is in turn H-bonded to an aspartate (Asp102).

Similar effects might be operative in metallo-enzymes. Indeed, the existence of conserved structural motifs involving metal ligands H bonded to surrounding amino acids[3,6,7] suggests that residues further away from the metal might play a pivotal role in enzymatic activity. Thus, the chemical properties of the metal sites might be affected by the surrounding protein matrix by means of outer-shell amino acid residues that interact with the metal-bound ligands through hydrogen bond networks.[3,6,7]

Zn-based enzymes constitute a typical example in this respect. Inspection of the Protein Data Bank database[8] shows that, in the majority of cases, histidine ligands are hydrogen-bonded to glutamate and aspartate, forming a Zn−His−carboxyl(ate) triad (Chart 1 and Table 1) (refs 7, 9, and 10). The carboxyl is in turn hydrogen-bonded to a hydrogen-bonding donor (H−X in

CHART 1

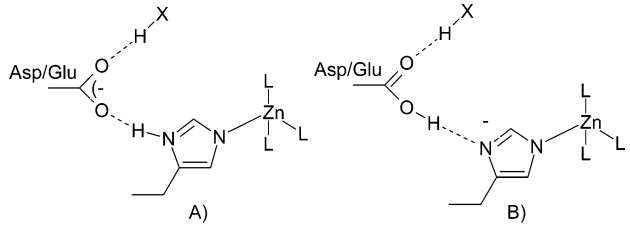

Chart 1), usually a water molecule (X = OH) or a backbone amide group (X = N−H). Through this "outer shell" hydrogen-bonding network, the protein scaffold may modulate the Lewis base properties of the histidine ligand and influence the catalytic properties of the enzyme by affecting the pK_a of metal-bound ionizable groups.[9,10] Thus, the presence of the H−X/Asp/His assembly may be important for the metal binding properties.

Here we address this issue by carrying out density functional theory calculations on the NAD^+/NADH-dependent enzyme (LADH, EC 1.1.1.1), which features the Zn−His−Asp−water motif at the active site shown in Figure 1. LADH catalyzes the oxidation of primary and secondary alcohols, which is performed by the NAD+ cofactor. This system appears to be suitable for this investigation as (i) LADH is one of the most studied Zn-based enzymes at the ab initio level,[11,12] so that an extensive comparison can be made with previous work, and (ii) the role of the Asp group binding to the His−Zn moiety has already been suggested by several experiments. Indeed, Asp49 is fully conserved in the mammalian isoenzymes[13−16] as well as in those of higher plants[14,15] and fungi.[16,17] Mutation of Asp49 to Asn

* To whom correspondence should be addressed. Phone: +39-040-3787407. Fax:+39-040-3787-528. E-mail: carloni@sissa.it.
† Università di Firenze.
‡ International School for Advanced Studies (SISSA/ISAS) and INFM-DEMOCRITOS Center for Numerical Simulation.
§ CSCS-Centro Svizzero di Calcolo Scientifico.
|| European Laboratory for Non linear Spectroscopy (LENS).
⊥ Università di Siena.
Physical Chemistry, ETH Hönggerberg HCI.

10.1021/jp027567h CCC: $25.00
Published on Web 06/20/2003

TABLE 1: Zinc Enzymes Containing the Zn−His−(Asp,Glu)−HX Arrangement[a]

PDB entry	name	N His-O(Asp,Glu), Å	O(Asp,Glu)-X(O−WAT), Å	protein type	resolution, Å	ref
1HET	liver alcohol dehydrogenase	2.8	2.7	oxidoreductase	1.0	2
1XSO	Cu, Zn superoxide dismutase	2.8	2.8	oxidoreductase	1.49	50
1EZM	elastase	2.7	3.0	hydrolase	1.5	51
1AH7	phospholipase	4.7	2.8	hydrolase	1.5	52
2CTB	carboxypeptidase-A	2.7	2.8	hydrolase	1.5	53
2CBA	carbonic anhydrase II	2.6	2.8*	lyase	1.54	54
8TLN	thermolysin	2.7	2.8	hydrolase	1.6	55
1VHH	sonic hedgehog	2.7	2.6	signaling prot.	1.7	56
1XJO	aminopeptidase	2.9	2.8	hydrolase	1.75	57
1TON	tonin	2.7	3.0*	hydrolase	1.8	58
1SLM	stromelysin-1	2.9	2.7**	hydrolase	1.9	59
1AZV	Cu, Zn superoxide dismutase	2.6	2.7	oxidoreductase	1.9	60
1CLC	endoglucanase	2.6	2.6	hydrolase	1.9	61

[a] Of the 26 nonhomologous structures of zinc enzymes resolved better than 1.9 Å present in the PDB database,[46] 13 (50%) contain the Zn−His−(Asp,Glu)−HX moiety. Here we report their PDB entry, and the distances between the carboxyl oxygen and the Nδ of the histidine, and between the other carboxyl oxygen and the water oxygen or backbone NH (*) or Arg NH_2 (**) groups.

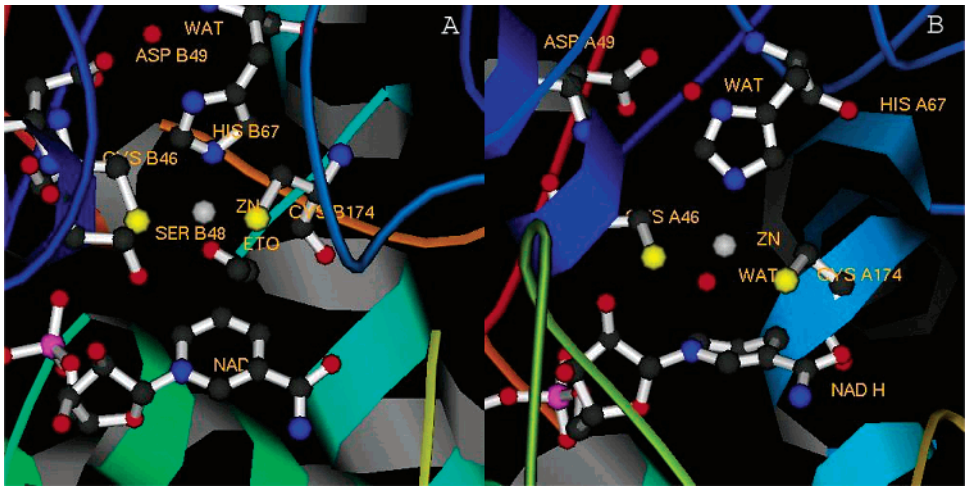

Figure 1. Structure of the HLAD active sites where a Zn(II) ion is bound.[4] The active site features the NAD^+ cofactor and a Zn ion (represented as a sphere) bound to His67, Asp49, Cys174, and either an alcoholate in the complex with the substrate (ternary complex, A) or a water molecule, in the free enzyme (binary complex, B). Figure prepared with the program MOLMOL.[62]

in the isoenzyme from *S. cerevisiae* decreased the catalytic efficiency by 3 orders of magnitude.[18]

The X-ray structures of the enzyme in the complex with NAD^+ and/or with substrate analogues have been determined at high resolution by X-ray crystallography.[2,19,20] In the active site, the zinc ion is bound to two cysteinates, to a histidine, and to the substrate analogue. The Zn-bound alcohol transfers a hydride ion to the NAD+ cofactor. A Zn-bound water molecule, which has been recently detected in the structure of the enzyme/NADH adduct, might assist in this process.[2]

In this paper, we have carried out calculations on two different structural models: in the first, which represents the LADH/NAD^+/substrate analogue ternary complex, the Zn has a *normal* tetrahedral coordination; in the second, which is a binary complex between LADH and NADH, the tertrahedral coordination of the zinc is distorted by the formation of an adduct between a metal bound hydroxide and NADH as reported in the paper by Meijers et al.[2] In this latter case, the zinc atom, the two sulfur atoms of the binding cysteines, and the nitrogen of the histidine are almost coplanar, leaving enough space to allow Zn to bind five ligands, including the NADH bound water molecule and substrate binding the zinc.

Our results suggest that in both complexes the Asp/water moiety significantly affects the structural and electronic properties of the active site, and it might therefore play a role in the enzymatic mechanism.

Methods

Structural Models. The starting models of our quantum-chemical calculations were based on the structure of the F93W LADH/NAD+/substrate analogue (trifluoroethanol) ternary complex, which has been solved by X-ray diffraction at 2.0 Å resolution (Protein Data Bank[21] entry: 1AXE[1]). 1AXE is the only enzyme/substrate-analogue (trifluoroethanol)/NAD^+ complex whose 3-D structure has been determined[1] (Figure 1A). Calculations were also carried out on the structure by Meijers et al.,[2] where, altough the substrate analogue is lacking (i.e., it is a binary complex), the resolution is the highest to date (1.0 Å). In this structure, an adduct between a metal-bound water and NADH was observed (Figure 1B).

Complexes at several levels of sophistication were considered. (i) In the case of the enzyme/substrate/NAD+ complex, the simplest model used is **A**, which includes the Zn(II) cation and its first-shell coordination ligands (His67, Cys46, Cys174, and ethanolate), the NAD^+ cofactor bound at the active site, and Ser48 H-bonded to NAD^+ (Figure 2). His67 was modeled as an imidazoyl that accounts for most of the important chemical effects[22−25] such as π-electron polarizability and π-donor capability.[26] Cys46 and Cys174 were modeled as methyl-thiolates. These groups were assumed to be deprotonated consistently with previous proposals[27] and with the observation that a significant decrease in the pK_a of methyl-thiolates occurs when they are bound to zinc.[28] The ethanol substrate was

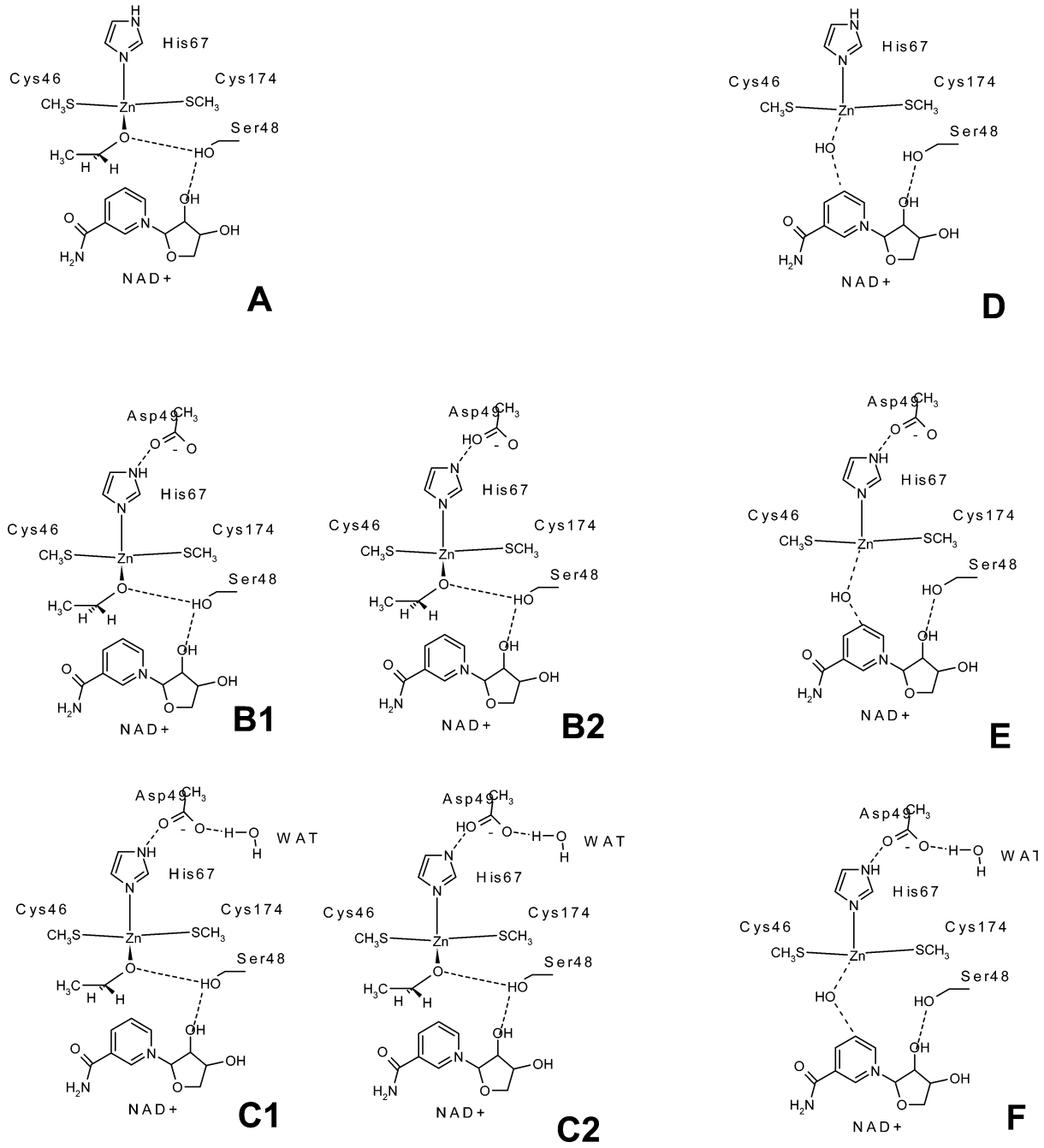

Figure 2. Models of the LADH active site used in the quantum-chemical calculations.

obtained by replacing the fluorine atoms of tri-fluoro-ethanol found in the crystal structure with hydrogens. Only the deprotonated (ethanolate) form of ethanol was considered in the calculations, as kinetic experiments have shown that the pK_a of the alcohol in this complex should be around 6.[29b] Finally, NAD^+ and Ser48 were modeled as nicotinamide nucleoside and ethanol, respectively. (ii) Complexes **B1/B2** are the same as **A** except that Asp49, modeled as acetate, is included. The His67 proton was either maintained on the histidine Nδ atom (**B1)** or located on the Asp49 carboxylate oxygen (**B2)**. (iii) Complexes **C1/C2** are the same as **B1/B2**, respectively, with the exception of one water molecule (WAT, in Figure 2) that is added to the model. WAT is a highly ordered water molecule present in most of the X-ray structures of the native enzyme and of its variants reported so far.[29a] Besides Asp49, WAT is H-bonded to Gly44, to His67, and to Glu68 (Figure 1SI). To estimate the effect of the latter three hydrogen bonds, omitted in the model complexes, we performed quantum-chemical calculations on the WAT/Gly44/Glu68 complex. The electron density turned out to be very similar to that of the isolated WAT, indicating that the polarization induced on the Gly44 H-bond acceptor is almost perfectly counterbalanced by the effect of His67 and Glu68 H-bond donors. Thus, omission of the latter interacting groups in complexes **A1**−**A2** is not expected to alter our results significantly. The overall charges of models **A**, **B1**−**B2**, and **C1**−**C2** were 0, −1, and −1, respectively.

In case of the binary complex, the calculations were done on models **D**, **E**, and **F**, in which we included the same residues as in **A**, **B1**, and **C1** except that a hydroxy group replaces the substrate and NADH is modeled instead of NAD^+ (Figure 2).

Quantum Chemistry. Our computational tool was gradient-corrected density functional theory; Becke[30] and Lee−Yang−Parr[31] gradient corrections were used for the exchange and correlation functional. The valence shell electrons were treated

CHART 2

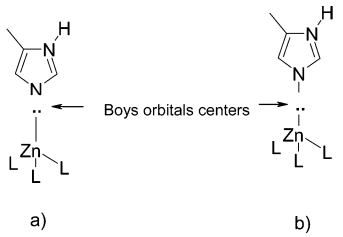

explicitly, and the core-valence shell interactions were described by pseudopotentials. For Zn, the d^{10} semi-core electrons were considered explicitly in the calculations. As structural properties may be sensitive to the basis set used,[11] we energy-minimized the structures **A**, **B1**−**2**, and **C1**−**2** with two kinds of basis sets: plane waves (PW) and Gaussian (G) type orbitals. The plane wave basis was expanded up to a cutoff of 70 Ry, with Martins-Troullier pseudopotentials[32] (code used: CPMD[33]). This setup was shown to reproduce accurately the structural properties of the Zn coordination polyhedron in human carbonic anhydrase II.[34] The Gaussian type orbitals were expanded in triple-ζ valence basis sets with one additional set of d-type functions (TZVP); the charge was expanded in plane waves to 120 Ry with Goedecker pseudopotentials[35] (code used: Quickstep[36]). For the calculations made on the enzyme/water/NADH complex, only the plane-wave basis set was used.

Geometry optimizations were performed using a combined quenched dynamics[25] and direct inversion of the iterative subspace method[37,38a] up to a gradient on the nuclear position of 10^{-4} a.u. Constraints on the position of the Zn ion, of the terminal methyl carbon atoms, and of the NAD^+ sugar carbon C1′ were used in all of the calculations to simulate the movement restraint imposed by the protein frame, following a common procedure in the literature.[38b]

Some calculations were carried out on model **C1** in the presence of the electrostatic potential of the solvated protein, calculated as in ref 39. To this end, a structural model of the protein/water system was built according to the following procedure. First, the WAT/ NAD^+/ethanol ternary complex was built from the F93W/ NAD^+/ethanol structure[1] by replacing Trp93 with a Phe residue. Only the atoms of the monomer were included in the calculations. The His residues were treated as in ref 11. A shell of water molecules (8 Å thick) was added using the EDIT module of the AMBER[40] suite of programs. The position of water molecules and the hydrogen atoms were energy-minimized using the SANDER module of AMBER.[40] The calculations were based on the standard AMBER force field parameters[41] for the protein/water system; for the cofactor (NAD^+), the standard procedure for calculating the charges, based on the RESP algorithm,[42] was adopted. The charges and atom types for NAD^+ and ethanolate are reported in Table 2 of the Supporting Information.

For the ethanolate, zinc, and cysteinates attached to zinc, we used the charges and force field of ref 11.

The chemical bonding was characterized in terms of centers of Boys orbitals.[43] These centers represent chemical concepts such as the Lewis doublet and the electron lone-pairs: Chart 2a shows, as an example, the center that represents the Lewis doublet of the Zn−Nϵ2(His67) bond. Changes in the chemical environment can be monitored in terms of bond ionicity indexes (BI), which are related to *shifts* of Boys orbitals upon a change in the chemical environment.[44] Changes in BIs have been found to be related to changes in the polarity of the chemical bonds.[44]

The change of electronic density on passing from one model complex to another was calculated as the difference in electronic density between the two models, as in ref 45.

Results

In this section, we first investigate the structural and electronic properties of the enzyme/substrate/NAD+ ternary complex by ab initio calculations using both plane waves (PW) and Gaussian (G) basis sets. This complex features a tetracoordinated Zn ion. Subsequently, we investigated the influence of second-shell ligands on the enzyme/hydroxyl-NADH binary complex using the same computational setup.

Ternary Complex. To estimate the influence of Asp49 and WAT on the metal complexes, we carried out quantum chemical calculations on models of increasing complexity. The simplest is **A**, which comprises the zinc coordination shell, the cofactor, and Ser48 (Figure 2). Overall, the calculated structural parameters of model **A** are in fair agreement with the experimental data.[1] However, a discrepancy is found for the calculated Zn−Nϵ2(His67) distance in model **A**, which is substantially longer than that determined in the X-ray structures that range between 2.12 and 2.14 Å (more than 0.1 Å shorter than in **A**, Table 2a). The same discrepancy is also found between the X-ray structures and previous ab initio quantum-chemistry calculations on models of similar or smaller size, using computational setups different from those used here[11,12] (Table 2a). This suggests that one or more of the interacting groups that influence the structure of the metal binding site are missing.

Asp49, which H-bonds to His67, was included in complexes **B1** and **B2**, which differ in the location of one proton. In **B1**, the proton is located on the Nδ1(His67) atom, and in **B2**, it is on the carboxylic oxygen of Asp49 (Figure 2). The energies of the two protomers turned out to be very similar (Table 3) using both PW and G basis sets. Thus, the structural analysis was carried out for both **B1** and **B2**. The calculated structural features are in better agreement with the experimental data than those of **A** (Table 2a). In particular, the Zn−Nϵ2(His67) distance in **B1** is shorter than in **A**, and reproduces the X-ray structure fairly well.

The structural change is accompanied by a change in the electronic structure. Addition of Asp49 causes a transfer of negative charge via His67 to the zinc ion and to the ethanolate substrate: Figure 3a shows the difference in the electronic density between model **A** and model **B1**. This can be interpreted in terms of a simple electrostatic model: the inclusion of the Asp49 negative charge polarizes the His67 π system (Figure 3c) which in turn donates electron density to zinc and, to a lesser extent, to the substrate. Consistently, the Boys orbital center located at the Nϵ2(His67) atom, which provides a vivid picture of a nitrogen lone pair (see Methods), moves significantly toward zinc (Table 4 and Chart 2). The inclusion of Asp49 in the model also causes a significant increase in the polarity of the ethanolate C−H bond, represented by the increase in the bond ionicity index (BI) when going from model **A** to **B1**−**B2.** A small but sizable effect is also present on the NAD^+ ring (Figure 4 of the Supporting Information).

The inclusion of a water molecule H-bonded to Asp49 (WAT in complexes **C1**−**C2**, Figure 2) causes a slight improvement in the structural properties of the model: several structural parameters are in better agreement with experimental data than those of complexes **B1**−**B2** (Table 2). The most relevant effect of the WAT H-bond to Asp49 is to increase the stability of **C1** with respect to **C2**. This finding is obtained with both P and G basis sets (Table 3). Comparison with the **B1**/**B2** protomers

TABLE 2: Selected Structural Parameters of Model Complexes Used in the Quantum-Chemical Calculations (Figure 2, part A, and Figure 3, part B)

Part A[a]

		distances						angles subtended at the Zn atom						
		Zn−N	Zn−S1	Zn−S2	Zn−O1	O1−O2	H−NAD	∠S1−S2	S1−N	S2−N	S1−O1	S2−O1	N−O1	RMS
PW	C1	2.11	2.42	2.32	2.09	2.57	2.59	124	108	112	102	104	104	0.18
	C2	2.11	2.42	2.35	2.11	2.57	2.59	122	111	112	104	103	102	0.21
G	C1	2.09	2.39	2.34	2.05	2.54	2.57	122	111	113	104	104	101	0.19
	C2	2.06	2.40	2.35	2.07	2.53	2.61	120	111	114	104	104	101	0.22
PW	B1	2.14	2.41	2.33	2.03	2.50	2.40	122	107	114	104	105	103	0.19
	B2	2.09	2.46	2.35	2.11	2.55	2.54	119	110	114	101	103	108	0.22
G	B1	2.13	2.34	2.39	2.04	2.51	2.41	126	113	107	103	104	102	0.19
	B2	2.08	2.39	2.37	2.08	2.53	2.48	123	109	113	103	103	103	0.23
PW	A	2.25	2.36	2.31	2.06	2.57	2.56	137	103	108	102	100	104	0.26
(1)		2.27	2.40	2.40	1.92									
(2)		2.18	2.34	2.35	2.12									
(3)		2.14	2.32	2.23	2.26	2.56		130	106	113	103	104	94	
(4)		2.13	2.13	2.29	2.07	2.54	2.27	116	106	114	112	111	96	
(5)		2.12	2.25	2.27	2.25	2.66		130	116	104	103	105	93	

Part B[b]

		distances				angles subtended at the Zn atom						
		Zn−N	Zn−S1	Zn−S2	Zn−O1	∠S1−S2	S1−N	S2−N	S1−O1	S2−O1	N−O1	RMS
PW	F	2.11	2.28	2.31	2.29	135	109	110	101	82	117	0.10
PW	E	2.16	2.30	2.31	2.29	133	107	106	102	83	115	0.12
PW	D	2.19	2.27	2.33	2.27	138	110	108	98	86	116	0.15
1HET		2.09	2.28	2.30	2.29	133	111	108	100	82	113	

[a] The parameters were calculated using both plane-wave (PW) and Gaussian (G) basis sets. Comparison is made with previous calculations[2] and structural data.[3] Distances and RMSD are in Å, and angles (∠) are in degrees. The RMS was calculated between the non-hydrogen atoms of the model complexes and the corresponding atoms in the LADH/2 (1S,3S)3-butylthiolane 1 oxide/NAD+ ternary complex.[20] We have compared our structural data to the HLAD/3-butylthiolane complex and not to that with trifluorethanol because the former structure was resolved at a better resolution. N is ϵ-nitrogen of His67, S1 is the sulfur atom of Cys174, S2 is the sulfur atom of Cys46, O1 is the ethanolate oxygen, O2 is the oxygen of Ser48, H−NAD is the distance between the ethanolate CH_2 hydrogen and the nearest carbon atom on NAD^+. [b] The parameters were calculated using a plane-wave (PW) basis set. Comparison is made with structural data. Distances and RMSD are in Å, and angles (∠) are in degrees. The RMS was calculated between the non-hydrogen atoms of the model complexes and the corresponding atoms in LADH/hydroxide/NADH ternary complex. N is ϵ-nitrogen of His67, S1 is the sulfur atom of Cys174, S2 is the sulfur atom of Cys46, O1 is the hydroxide oxygen.

TABLE 3: Energy Differences (kcal/mol) between the Protomers B1/B2 and C1/C2

	PW	G
E(B1)−E(B2)	−0.35	−0.5
E(C1)−E(C2)	−3.5	−4.05

indicates that the WAT interaction stabilizes the protonation of His67 Nδ1. The geometrical parameters of the complex **C1** have smaller RMS deviations from the X-ray structure than those of **C2** (Table 2a**)**.

The effect of WAT on the polarization of the His67 is smaller and the opposite of that due to Asp49 alone (Figure 3b). This occurs presumably because of the electron-withdrawing effect of WAT toward Asp49 which, in turn, causes a decrease in the electronic density transferred to His67. As expected, the effect of WAT on the electronic structure of the substrate is negligible (Figure 3 and Table 4). In addition, the effect on the energetics of the substrate deprotonation reaction is negligible and almost within the error of the method (Table 4). We conclude therefore that in the enzyme−substrate complex His67 is protonated at Nδ1 and that both Asp49 and WAT affect the structural and electronic properties of the system.

The effects due to the atoms of the protein not included in our largest model (models **C1**/**C2**) were taken into account by means of the external field of the protein[39]. The mean displacement of the centers of the Boys orbitals turned out to be as small as 0.005 Å.

We conclude that the effects of environment appear not to play a major role in influencing the electronic properties of the complex.

Binary Complex. Also in this case, in complex **D**, the calculated Zn−Nϵ2(His67) turns out to be larger than the experimental value (2.20 Å vs 2.09 Å, Table 2b). Inclusion of Asp49 (model E) and WAT (model F) is also here crucial in order to reproduce the structural properties correctly (Table 2b). The agreement between model F and experimental structural data (Table 2b, overall RMS 0.10 Å) is even better than that obtained for model C.

As in the ternary complex, (i) Asp49 polarizes the metal center significantly, as clearly seen from the plot of the electronic density difference in Figure 4 of the Supporting Information, and (ii) the presence of WAT stabilizes the protonated form of His67 (Table 4 of the Supporting Information).

We conclude that both in the tetra or penta-coordination, and in the presence or in the absence of the substrate, the outer-shell ligands WAT and Asp49 play a role in the structural and electronic properties of the active site.

Discussion

First principles quantum chemical calculations based on both localized (G) and delocalized (PW) basis sets were carried out for models of increasing complexity representing the LADH ternary complex (Figure 2). Calculations on complex **A** (Figure 2), which includes the active site zinc-ligand complex, the cofactor, and Ser48 interacting with it are in good agreement with experimental data. However, they turn out not to be able to reproduce the structural properties of the Zn−Nϵ2(His67) bond. This result is in line with previous quantum-chemical

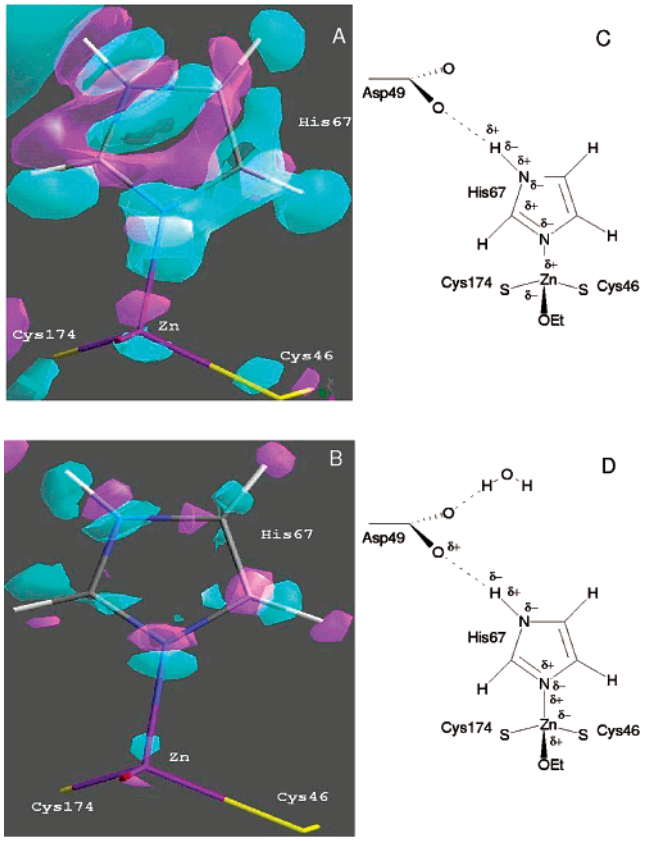

Figure 3. Electron density differences between model **A** and **B1** (a) and model **B1** and **C1** (b). Magenta surfaces refer to +0.001 (a) and +0.0005 (b) $e^-/(a.u.)^3$ values, respectively; blue to −0.001 (a) and −0.0005 (b) $e^-/(a.u.)^3$ $e^-/(a.u.)^3$. (c)−(d) Schematic representation of polarization effects in (a) and (b), respectively.

TABLE 4: Electronic Properties of the Complex[a]

	Zn−Nϵ(His67)							
	distances, Å				bond ionization indexes			
model	C	B1	B2	A1	C	B1	B2	A1
Zn−BC	1.643	1.668	1.581	1.670	0.139	0.137	0.126	0.152
BC−N	0.477	0.470	0.499	0.450	−0.139	−0.137	−0.126	−0.152

CH bond	B. I.
methane[44]	0.0070
ethanol	0.0079
ethanolate	0.0447
ethanolate in **C1**	0.0282
ethanolate in **B1**	0.0286
ethanolate in **A**	0.0236

[a] Top: Zn−Nϵ(His67) bond. Distances between Boys Orbitals centers (BC) and the atoms forming the bond and bond ionicity (BI) indexes. Bottom: CH bond. BI indexes of CH_2 in methane and ethanol in different chemical environments. BI in ethanol and ethanolate in a vacuum can be taken as a reference for the hydride character of the bond.

calculations on similar or smaller basis sets (Table 2a and references therein)

Calculations on complex **B** (Figure 2), which include the Asp49 side chain, show that Asp49 affects the structural and electronic properties of the complex (Table 2a). Indeed, the hydrogen bond between Asp49 and His67 increases the electron density on the His67 Nϵ atom. This in turn strengthens the Zn−Nϵ coordination bond. Furthermore, Asp49 polarizes His67, which in turn polarizes the metal ion and the alcoholate oxygen (Figure 3). The polarization of Asp49 on the His67−Zn−substrate complex (Figure 3a) increases the hydride character of the alcohol methylene hydrogen that is transferred to NAD^+ during the oxidation phase (Table 4). Asp49 therefore plays a role in the geometry of the active site and the balance of electron density on the zinc ion. The inclusion in our model of the WAT water molecule (models **C1**/**C2** in Figure 2) provides an even better agreement with the X-ray structure (Table 2a) and renders unfavorable the deprotonation of His67 by Asp49, leaving the hydrogen on the histidine Nδ1 atom. This finding is in agreement with the experimental results of Bertini et al.[63] that do not find evidence for His67 deprotonation in the ternary complex. Instead, this finding contrasts with the proposal, based either on speculation on the position of the hydrogen in the X-ray structure[29a] or on ab initio calculations,[46] that Asp49 acts as a proton acceptor rather than a hydrogen-bond acceptor toward His67. The latter calculations, carried out on model complexes which did not include either WAT or any other X−H group (Chart 1), showed that in absence of these outer-shell ligands, the imidazole−acetate moiety in the active site of the enzyme is energetically less stable than the imidazolate−acetic acid moiety. Consistently, we also find that the absence of WAT renders the protonation of Asp49 possible (Table 3; Figure 2b1), which in turn affects the polarization of His67, Zn, and the substrate (Figure 3b).

WAT also has polarizing effects (albeit an order of magnitude smaller than those of Asp) on the zinc ion through Asp49 and His67. This provides evidence that inclusion of the water molecule may also be important for describing the electronic structure of the enzyme active site.

Similar results are found for the enzyme/NADH binary complex (Figure 1B): also in this case, the correct geometry of the His−Zn bond is reproduced only when Asp49 is included in the model, and the presence of WAT stabilizes the protomer in which His67 is protonated relative to that in which His67 is deprotonated.

In conclusion, our calculations suggest that second (Asp49) and third-shell (WAT) ligands affect the structure, electronic properties, and energetics of the LADH active site. At the speculative level, these results might help explain, at least in part, the loss of catalytic activity and the structural rearrangement of the active site that were indirectly observed in the D49N[18] mutant: indeed, the replacement of Asp49 by a residue not charged such as Asn might affect the structural and electronic properties of the LADH active site, which in turn might play a role in the enzymatic reaction.

Acknowledgment. The authors thank U. Roethlisberger for providing the Zn pseudopotential. Financial support by MURST-COFIN is also acknowledged.

Supporting Information Available: Tables 1SI and 2SI and Figures 1SI−4SI. This material is available free of charge via the Internet at http://pubs.acs.org.

References and Notes

(1) Bahnson, B. J.; Colby, T. D.; Chin, J. K.; Goldstein, B. M.; Klinman, J. P. *Proc. Natl. Acad. Sci. U. S.A* **1997**, *94*, 12797−12802.

(2) Meijers, R.; Morris, R. J.; Adolph, H. W.; Merli, A.; Lamzin, V. S.; Cedergren-Zeppezauer, E. S. *J. Biol. Chem.* **2001**, *276*, 9316−9321.

(3) Chakrabarti, P. *Protein Eng.* **1990**, *4*, 57−63.

(4) Fersht, A. *Structure and mechanism in protein science: a guide to enzyme catalysis and protein folding*; W. H. Freeman: New York, 1999.

(5) Dugas, H. *Bioorganic Chemistry*, Springer: New York, 1996.

(6) Christianson, D. W. *Adv. Protein Chem.* **1991**, *42*, 281−355.

(7) Christianson, D. W.; Cox, J. D. *Annu. Rev. Biochem.* **1999**, *68*, 33−57.
(8) Bernstein, F. C. l.; Koetzle, T. F.; Williams, G. J. B. *J. Mol. Biol.* **1999**, *112*, 535−542.
(9) Christianson, D. W.; Alexander, R. S. *J. Am. Chem. Soc.* **1989**, *111*, 6412−6419.
(10) Christianson, D. W.; Alexander, R. S. *Nature* **1990**, *346*, 225.
(11) Ryde, U. *Proteins: Struct. Funct. Genet.* **1995**, *21*, 40−56.
(12) Ryde, U. *J Comput. Aided Mol. Des.* **1996**, *10*, 153−164.
(13) Jornvall, H.; Persson, B.; Jeffery, J. *Eur. J. Biochem*. **1987**, *167*, 195−201.
(14) Chang, C.; Meyerowitz, E. M. *Proc. Natl. Acad. Sci. U.S.A.* **1986**, *83*, 1408−1412.
(15) Dennis, E. S.; Sachs, M. M.; Gerlach, W. L.; Finnegan, E. J.; Peacock, W. J. *Nucleic Acids Res.* **1985**, *13*, 727−743.
(16) Jornvall, H.; Eklund, H.; Branden, C.-I. *J. Biol. Chem.* **1978**, *253*, 8414−8419.
(17) McKnight, G. L.; Kato, H.; Upshall, A.; Parker, M. D.; Saari, G.; O'Hara, P. J. *EMBO J.* **1985**, 2093−2099.
(18) Ganzhorn, A. J.; Plapp, B. V. *J. Biol. Chem.* **1988**, *263*, 5446−5454.
(19) Al-Karadaghi, S.; Cedergren-Zeppezauer, E. S.; Petrantos, K.; Hovmoller, S.; Terry, H.; Dauter, Z.; Wilson, K. S. *Acta Crystallogr.* **1994**, *D50*, 793−807.
(20) Cho, H.; Ramaswamy, S.; Plapp, B. V. *Biochemistry* **1997**, *36*, 382−389.
(21) Berman, H. M.; Westbrook, J.; Feng, Z.; Gilliland, G. L.; Bhat, T. N.; Weissig, H.; Shindyalov, I. N.; Bourne, P. E. *Nucleic Acids Res.* **2000**, *28*, 235−242.
(22) Venanzi, C. A.; Weinstein, H.; Corongiu, G.; Clementi, E. *Int. J. Quantum Chem., Quantum. Biol. Symp.* **1982**, 355−365.
(23) Tang, C. C.; Davalian, D.; Huang, P.; Breslow, R. J. *J. Am. Chem. Soc.* **1978**, *100*, 3918−3922.
(24) Brown, R. S.; Salmon, D.; Curtis, N. J.; Kusuma, S. *J. Am. Chem. Soc.* **1982**, *104*, 3188−3194.
(25) Carloni, P.; Blochl, P. E.; Parrinello, M. *J. Phys. Chem.* **1995**, *99*, 1338−1348.
(26) Demoulin, D.; Pullman, A. *Theor. Chim. Acta* **1978**, *49*, 161−181.
(27) Vanhommerig, S. A. M.; Meier, R. J.; Sluyterman, L. A.; Meijer, E. M. *J. Mol. Struct.: THEOCHEM* **1996**, *364*, 33−43.
(28) El Yazal, J.; Pang, Y. P. *J. Phys. Chem. B* **1999**, *103*, 8773−8779.
(29) (a) Hurley, T. D.; Bosron, W. F.; Stone, C. L. *J. Mol. Biol.* **1994**, *239*, 415−429. (b) Maret, W.; Makinen, M. W. *J. Biol. Chem.* **1991**, *266*, 20636−20644.
(30) Becke, A. *Phys. Rev. A* **1988**, *38*, 3098−3100.
(31) Lee, C.; Yang, W.; Parr, R. G. *Phys. Rev. B* **1988**, *37*, 785−789.
(32) Troullier, N.; Martins, J. L. *Phys. Rev. B* **1991**, *43*, 1943−2006.
(33) CPMD, Version 3.0h: Hutter, J.; Marx, D.; Focher, P.; Tuckerman, M.; Andreoni, W.; Curioni, A.; Fois, E. U.; Roetlisberger; Giannozzi, P.; Deutsch, T.; Alavi, A.; Sebastiani, D.; Laio, A.; VandeVondele, J.; Seitsonen, A.; Billeter, S.; et al. Copyright: IBM Corp.; Copyright: Max Planck Institute, Stuttgart. Program available at the Web page www.cpmd.org.
(34) Rothlisberger, U. *Ab initio and hybrid molecular dynamics simulations of the active site of Human Carbonic Anhydrase II: A test case study*; Gao, J., Thompson, M. A., Eds.; American Chemical Society: Washington, DC, 1998.
(35) Goedecker, S.; Teter, M.; Hutter, J. *Phys. Rev. B* **1996**, *54*, 1703−1710.
(36) Lippert, G.; Hutter, J.; Parrinello, M. *Theor. Chem. Acc.* **1999**, *103*, 124−140.
(37) Pulay, P. *Chem. Phys. Lett.* **1980**, *73*, 393−398.
(38) (a) Csazar, P.; Pulay, P. *J. Mol. Stuct. (THEOCHEM)* **1984**, *114*, 31−34. (b) Díaz, N.; Suárez, D.; Merz, K. N., Jr. *J. Am. Chem. Soc.* **2001**, *123*, 9867−9879.
(39) Piana, S.; Carloni, P. *Proteins: Struct., Funct., Genet.* **2000**, *39*, 26−36.
(40) Case, D. A.; Pearlman, D. A.; Caldwell, J. W.: Cheatham, T. E.; Ross, W. S.; Simmerling, C. L.; Darden, T. A.; Merz, K. M.; Stanton, R. V.; Cheng, A. L.; Vincent, J. J.; Crowley, M. F.; Ferguson, D. M.; Radmer, R. J.; Singh, U. C.; Weiner, P. K.; Kollman, P. A. *AMBER* [5.0]; University of California: San Francisco, CA, 1997.
(41) Cornell, W. D.; Cieplack, P.; Bayly, C. I.; Gould, I. R.; Merz, K. M.; Ferguson, D. M.; Spellmeyer, D. C.; Fox, T. *J. Am. Chem. Soc.* **1995**, *117*, 5179−5197.
(42) Bayly, C. I.; Cieplack, P.; Cornell, W. D.; Kollman, P. A. *J. Phys. Chem.* **1993**, *97*, 9620−9631.
(43) Silvestrelli, P. L.; Marzari, N.; Vanderbilt, D.; Parrinello, M. *Solid State Commun.* **1998**, *107*, 7−11.
(44) Alber, F.; Folkers, G.; Carloni, P. *J. Phys. Chem.* **1999**, *103*, 6121−6126.
(45) Sulpizi, M.; Carloni, P. *J. Phys. Chem* **2000**, *104*, 10087−10091.
(46) El Yazal, J.; Roe, R. R.; Pang, Y. P. *J. Phys. Chem. B* **2000**, *104*, 6662−6667.
(47) Huang, C. C.; Lesburg, C. A.; Kiefer, L. L.; Fierke, C. A.; Christianson, D. W. *Biochemistry* **1996**, *35*, 3439−3446.
(48) Tainer, J. A.; Getzoff, E. D.; Beem, K. M.; Richardson, J. S.; Richardson, D. C. *J. Mol. Biol.* **1982**, *160*, 181−217.
(49) Banci, L.; Bertini, I.; Cabelli, D. E.; Hallewell, R. A.; Tung, J. W.; Viezzoli, M. S. *Eur. J. Biochem.* **1991**, *196*, 123−128.
(50) Djinovic Carugo, K.; Battistoni, A.; Carr, M. T.; Polticelli, F.; Desideri, A.; Rotilo, G.; Coda, A.; Wilson, K. S.; Bolognesi, M. *Acta Crystallogr. D* **1996**, *D52*, 176.
(51) Thayer, M. M.; Flaherty, K. M.; McKay, D. B. *J. Biol. Chem.* **1991**, *266*, 2864.
(52) Hough, E.; Hansen, L. K.; Birknes, B.; Jynge, K.; Hansen, S.; Hordvik, A.; Little, C.; Dodson, E.; Derewenda, Z. *Nature* **1989**, *338*, 357−360.
(53) Teplyakov, A.; Wilson, K. S.; Orioli, P.; Mangani, S. *Acta Cryst.* **1993**, *D49*, 534−540.
(54) Hakansson, K.; Carlsson, M.; Svensson, L. A.; Liljas, A. *J. Mol. Biol.* **1992**, *227*, 1192−1204.
(55) Holland, D. R.; Tronrud, D. E.; Pley, H. W.; Flaherty, K. M.; Stark, W.; Jansonius, J. N.; McKay, D. B.; Matthews, B. W. *Biochemistry* **1992**, *31*, 11310−11316.
(56) Hall, T. M.; Porter, J. A.; Beachy, P. A.; Leahy, D. J. *Nature* **1995**, *378*, 212−216.
(57) Greenblatt, H. M.; Almog, O.; Maras, B.; Spungin-Bialik, A.; Barra, D.; Blumberg, S.; Shoham, G. *J. Mol. Biol.* **1997**, *265*, 620−636.
(58) Fujinaga, M.; James, M. N. *J. Mol. Biol.* **1987**, *195*, 373−396.
(59) Becker, J. W.; Marcy, A. I.; Rokosz, L. L.; Axel, M. G.; Burbaum, J. J.; Fitzgerald, P. M. D.; Cameron, P. M.; Esser, C. K.; Hangmann, W. K.; Hermes, J. D. *Protein Sci*. **1995**, *4*, 1966−1976.
(60) Hart, P. J.; Liu, H.; Pellegrini, M.; Nersissian, A. M.; Gralla, E. B.; Valentine, J. S.; Eisenberg, D. *Protein Sci.* **1998**, *7*, 545−555.
(61) Lascombe, M. B.; Souchon, H.; Juy, M.; Alzari, P. M. 1995.
(62) Koradi, R.; Billeter, M.; Wuthrich, K. *J. Mol. Graph.* **1996**, *14*, 51−32.
(63) Bertini, I.; Gerber, M.; Lanini, G.; Luchinat, C.; Maret, W.; Rawer, S.; Zeppezauer, M. *J. Am. Chem. Soc.* **1984**, *106*, 1826−1830.